AIAA SciTech Forum
6-10 January 2020, Orlando, FL
AIAA Scitech 2020 Forum

10.2514/6.2020-1793

CFD analysis of a Micro-rotor In Ground Effect

F. Rovere*, G. N. Barakos†, R. Steijl‡
CFD Laboratory, School of Engineering, University of Glasgow, G12 8QQ Glasgow, UK.

In this work computational fluid dynamics is validated using experimental results for a model rotor In Ground Effect. The paper concentrates on the evaluation and prediction of the performance of the rotors and on the outwash generated In Ground Effect. Finally, safety considerations in terms of outflow forces and particles in the flowfield are presented, comparing the results with other safety, distance based criteria. Using data of three different aircraft, scaling factors have been used to take into account the different size of the small-rotor studied and real case scenarios. The results show how heavier helicopters may generate the most dangerous situations, in terms of induced forces and presence of particles in a delimited area.

Nomenclature

Latin

a	=	Speed of sound, m/s
B	=	Ballistic coefficient, kg/m^2
c	=	Root blade chord, m
C_Q	=	Rotor torque coefficient, $C_Q = \frac{Q}{\frac{1}{2}\rho_\infty V_{tip}^2 \pi R^3}$
C_T	=	Thrust coefficient, $C_T = \frac{T}{\frac{1}{2}\rho_\infty V_{tip}^2 A}$
D	=	Rotor diameter, m
d_p	=	Particle diameter, μm
df_{PAXman}	=	$df_{PAXman} = \frac{1}{2}\rho V_{rad}^2 dA$, N/m
F_{PAXman}	=	$F_{PAXman} = \int_{A_{PAXman}} df_{PAXman}$, N
FoM	=	Figure of merit, $FoM = \frac{C_T^{3/2}}{2C_Q}$
g	=	Gravitional acceleration, m/s^2
h_{PAXman}	=	PAXman height scaled, m
h	=	Height above the ground,
M	=	Mach number, $M = V_{tip}c/a_\infty$
Q	=	Rotor torque, $N \cdot m$
r	=	Radial coordinate along blade span, m
R	=	Rotor radius, m
Re	=	Reynolds number, $Re = V_{tip}c/\nu_\infty$
S_{rotor}	=	Rotor disk area, m^2
U	=	Velocity x-component, m/s
V	=	Velocity y-component, m/s
u^*	=	Friction velocity, m/s
u_t^*	=	Threshold Friction velocity, m/s
V_{rad}	=	Velocity radial component, $V_{rad} = Ucos(\Psi) + Vsin(\Psi)$, m/s
v_i	=	Hover induced velocity, $v_i = \frac{\sqrt{(C_T)}}{2}$
v_{max}	=	Highest value of velocity radial component
T	=	Rotor thrust, N

Greek

*PhD Student, CFD Laboratory, School of Engineering, Email: federico.rovere@glasgow.ac.uk
†Professor, MAIAA, MRAeS, CFD Laboratory, School of Engineering
‡Senior Lecturer, CFD Laboratory, School of Engineering

θ_{75} = Collective pitch at three-quarter radius, deg
Ω = Rotor angular velocity, rad/s
Ψ = Local azimuth angle, deg
ρ = Density, kg/m^3
ν = Kinematic viscosity, m^2/s
τ_w = Wall shear stress, kg/ms^2

Subscripts and superscripts

∞ = Freestream value
tip = Blade tip value
p = Particle

Acronyms

CFD = Computational Fluid Dynamics
DVE = Degraded Visual Environment
IGE = In Ground Effect
$MUSCL$ = Monotone Upstream Centred Schemes for Conservation Laws
$MTOW$ = Maximum TakeOff Weight
OGE = Out of Ground Effect
PIV = Particle Image Velocimetry

I. Introduction

The ground has a strong influence on the induced wake, and on the performance of every type of rotor. This influence has been discussed in several works, considering from full-scale aircraft [1], to small-scale isolated rotors [2, 3]. In the first case, during experiments, it is possible to replicate the real operational conditions which the aircraft may encounter in an operational scenario. In general, however, measurement techniques used in full-scale experiments, lack high resolution, and cannot provide a detailed view of the phenomena involved. On the other hand, small-scaled studies can be performed in a laboratory, within a controlled environment and using high resolution measuring techniques, such as Particle Imagine Velocimetry (PIV). However, due to the limited size of the rotors, Reynolds number and Mach number are lower with respect to the full scale case, leading to some differences in the flowfield behaviour. As mentioned, ground influence has an effect on rotor performance. When rotors operate In Ground Effect (IGE), their thrust coefficient is higher with respect to the Out of Ground Effect (OGE) for a fixed amount of power, while the power coefficient decreases for a given thrust coefficient. The ground also has an effect on the wake of the lifting rotor, modifying its natural development. The wake direction changes from vertical (downwash) to horizontal (outwash) due to the ground effect and, the resulting flowfield has time-averaged characteristics similar to those of a wall-impinging jet [4]. These unsteady flowfields can generate potential hazards. In general, outflow can generate strong forces on ground personnel and structures in proximity to the rotor. [5]. A more dangerous situation can be generated by the interaction of the wake with a loose sediment bed. In this case particles can be uplifted from the ground and enter the flowfield. When the amount of particles is high, they can generate a cloud all around the aircraft which can spoil the visual of the pilot. This phenomenon is called brownout and it is one of the most severe Degraded Visual Environment (DVE) conditions. Brownout claimed many lives and aircraft during recent years, statistics about mishaps due to brownout are listed in [6]. Authors report that from 1990, US Air force lost 30 special operation aircraft and 60 crew members lost their lives due to mishaps related to brownout. Other NATO members experienced similar statistics. UK had 24 brownout mishaps in the period 2005-2009. The German defence force had more than 30 accidents due to dust and snow.

In this work Computational Fluid Dynamics (CFD) analysis is compared with experimental results of a test case investigated at University of Maryland by Lee et al. [2], and it involves the study of a small two-bladed rotor hovering IGE at different heights from the ground. Rotor performances were measured using a micro-mass balance while the flowfield data were obtained by 2D PIV. Performance of the same rotor was studied in [7] for an OGE case and, a previous work described the validation of CFD for this test case [8]. Once the CFD analysis is complete, the results were used to evaluate several safety considerations using force estimators on ground personnel and particle tracking. These

safety considerations are then compared with existing safety distances criteria, such as the 3 rotor diameter separation criteria for wake encounters [9, 10]. Initially, forces on ground personnel, properly scaled, are computed starting from the outflow velocities using the PAXman model [1, 5]. To obtain realistic full-scale scenarios, and compare the resulting forces with PAXman safety thresholds, scaling factors have been applied to velocities using three different aircraft, categorized in terms of weight. Scaling factors take into account differences in terms of thrust and tip velocity, however, they cannot take into account effects of different Reynolds numbers between small-scale and full-scale. To evaluate the presence of particles in the flowfield, the first step was to apply the uplift model to the ground. This way it is may possible to define where particles are likely to be uplifted. Using this information, it was possible to seed properly the ground and track the particles in the flowfield. Safety considerations are taking into account different type of rotors, delimiting different areas (in terms of size) where it is possible to operate safely. These considerations can be a starting point to evaluate safety constrains for future Personal Aerial Vehicle operations in highly populated areas.

II Numerical Methods

II.I CFD solver

HMB3 (Helicopter Multi-Block) [11, 12] is the solver used for all CFD calculations in this work. It solves the Unsteady Reynolds Averaged Navier-Stokes equations (URANS) in integral form with ALE formulation (Arbitrary Lagrangian Eulerian) for time-dependent domains (moving boundaries). URANS equations are discretized using a cell-centred finite volume approach on a multiblock structured grid. HMB3 uses the Osher [13] and Roe [14] approximate Riemann solvers to evaluate the convective fluxes, the viscous terms are discretized using second order central differencing. Third order accuracy in space is provided by the Monotone Upstream Centred Schemes for Conservation Laws (MUSCL) [15]. To avoid non-physical spurious oscillations HMB3 uses an alternative form of the Albada limiter [16] where large gradients are involved in computations, like in presence of shockwaves. An implicit dual time stepping method is employed in time-accurate simulations. Oversets grids (used in this work) [17] and sliding plane [18] methods are available in HMB3 to allow for the relative motion between mesh components, representing ground and rotor blade. Various turbulence models are available in HMB3, including one-equation, two-equation, three and four equations turbulent models. Large-eddy Simulation (LES), Detached-Eddy Simulation (DES) and Delay-Detached-Eddy Simulation (DDES) can also be used with HMB3. For this study two different turbulence model have been used: $k-\omega$ and $k-\omega$ SST [19], furthermore due to the low Reynolds numbers of the test cases few laminar simulations were also performed.

II.II Paxman model

Outflow generated by a lifting rotor IGE can affect ground staff operations. In the presence of strong winds people may have difficulties to walk or keep their eyes open, and in the worst case the outflow can make people fall. To define delimited safe areas around the rotor in terms of forces, the PAXman model has been used. The PAXman model was developed for military personnel as a reference area for the wind force calculation, it is based on the projection of a 6ft tall person immersed in the outwash. The details of the geometry of PAXman model are in Figure 1 as reported in [1, 5]. Using the reference area expressed by the polynomial representation of Figure 1, the distribution of the force produced by the outwash on the ground personnel is computed as proposed in [1]. To obtain comparable forces with the safety criteria, velocities were scaled using the blade tip velocity, listed in Table 2. The distribution of the force over the body was calculated as: $f_{paxman} = \frac{1}{2}\rho_{air}V_{rad}^2 x$, where ρ_{air} is density of the air, V_{rad} is the radial velocity and x is the horizontal coordinate of the PAXman model. The total force is the integral of the distribution of the force over the height of the PAXman model.

$$F_{paxman} = \int_{h_{PAXman}} f_{paxman} dz \tag{1}$$

According to [1, 5] the caution zone begins when the force acting on the PAXman is more than 80 lbf (335 N), and the hazard zone is defined after 115 lbf (510 N). To obtain comparable forces with the safety criteria, velocities have to be scaled using the blade tip velocity, listed in Table 2. This first scaling obtains velocities expressed in m/s, that can be later used, to compute the PAXman forces in N. However, a second scaling is necessary to take into account difference in C_T of the three different cases. A common reference value for outflow velocities is the hover induced velocity v_i, expressed as $v_i = \sqrt{C_T}/2$. To obtain the C_T^{fs} the aircraft is considered in hover flight, with the thrust equal to its

Maximum-Take-Off-Weight (MTOW). W_{MTOW}, V_{tip}, and S_{rotor} are specified in Table 2, while for the acceleration of gravity and for the air density the following values have been assumed: $g = 9.81 m/s^2$ and $\rho_{air} = 1.225 kg/m^3$.

$$C_T = \frac{W_{MTOW}}{0.5 \rho_{air} V_{tip}^2 S_{rotor}}. \tag{2}$$

It is possible, taking into account the effect of the different thrust coefficient to scale the velocities using the ratio of hover induced velocity between full-scale and small-scale cases. The scaling factor obtained is $\sqrt{\frac{C_T^{fs}}{C_T^{ss}}}$. This way, it is possible to estimate the outflow velocities generated by a full-scale rotor operating at the same high values of thrust coefficient of the scaled rotor. It is important to remember that the scaling factors considered in this work, do not take into account the effects of the different Reynolds numbers involved in the full and the small scale scenarios. Reynolds number affect the flowfield around the rotor, its features and its development in time. It is not possible to properly simulate brownout at full-scale, without taking into account a proper Reynolds number. However, this scaling method can be good a first estimation of forces and outflow velocities involved in a full-scale rotor scenario.

II.III Uplift Model of Loose Ground Particles

When the wake reaches the ground and interacts with the loose sediment, particles can be uplifted. To simulate this phenomenon, the Bangold model (see [20, 21]) has been used to simulate brownout in several works. The Bangold model has been developed within the sediment community to simulate the pick up of particles in river flows. In 2000 Shao et al. [22] proposed a simple formulation, based on Bangold model, that has been used in this work. It is a threshold model, based on the wall friction velocity $u_* = \sqrt{\frac{\tau_w}{\rho}}$. The threshold value depends on particle and fluid proprieties and on the gravity. It is computed as:

$$u_t^* = \sqrt{A(\frac{\rho_p}{\rho_{air}} g d_p + \frac{\beta}{\rho_{air} d_p})}, \tag{3}$$

where u_t^* is the threshold velocity, while A and β are coefficients: A=0.0123 β=3e-04 $\frac{kg}{s^2}$. The particle values, used in this work, are listed in Table 4, while for air and gravity the following values have been used: $\rho_{air} = 1.225 kg/m^3$ and $g = 9.81 m/s^2$. When $u^* > u_t^*$ the particle is uplifted and it is entrained the flowfield. Other causes can be involved in particles uplift that are not taken into account in this work. One of them is the "splash entrainment". Anytime an entrained particle hits the ground, it may launch more particles, if it has sufficiently high energy. Hit particles can gain enough kinetic energy to overcome cohesive forces and enter the flowfield [22, 23].

II.III Particle Tracking

Once particles are uplifted, and they enter the flowfield, this can lead to several dangerous situations. During brownout, particles generate a cloud all around the aircraft. Initially, particles are pushed away from the aircraft, but then they are reingested by the rotor. When this happens, particles are a source of danger for the aircraft and the crew. The main effect of the cloud is to spoil the visual of the pilot, potentially causing dynamic rollover or accidental collisions with objects in proximity of the aircraft. Other effects include the injection of the particles by the engines, and the damage caused by the particles impacting on the helicopter blades and fuselage. These phenomena involve, typically, smaller particles [24, 25], however, every kind of particle can be affected by the outflow, including sand, dust, snow and even small rocks. To proper define a safe zone from particles it is necessary to simulate their trajectory in the flowfield. Lagrangian and Eulerian modelling are the two approaches used in the numerical simulation of particle motion. The Lagrangian approach has been used in [26, 27] for brownout simulations. Using this approach the particles (or parcels of particles) are tracked through the field using the Newton's second law, and the local cloud properties are defined by their properties as they pass each point in the domain. On the other hand, in the Eulerian approach, the properties of the particles are assumed to be continuous within the flowfield. Thus, differential conservation equations are written, discretized, and solved for the properties of the cloud, e.g. [28, 29]. In this work, Tecplot^{TM} has been used for particle tracking.

The particles are driven by the flowfield velocities, and their positions in time are obtained by integrating their equation of motion. The integration method used is a second order Runge-Kutta , and the equation of particles motion

is the 2nd Newton law, considering aerodynamic and gravity forces:

$$m_p \mathbf{a}_p = 0.5\rho_f S C_d(\mathbf{u}_f - \mathbf{u}_p)||(\mathbf{u}_f - \mathbf{u}_p)|| - m_p \mathbf{g}, \tag{4}$$

it is possible to obtain the acceleration of the particle in terms of flowfield velocity and density, and particle propreties.

$$\mathbf{a} = \frac{0.5\rho_f(\mathbf{u}_f - \mathbf{u}_p)||(\mathbf{u}_f - \mathbf{u}_p)||}{B} - \mathbf{g} \tag{5}$$

In the above equation, B is the balistic coefficient, defined as $B = \frac{m_p}{SC_D}$ where m_p is the particle mass and S is the frontal area ($S = \pi(\frac{d_p}{2})^2$ for spherical particles). The particle proprieties used in this work, are listed in table 3. This equation is derived by the Newton second's law considering the same aerodynamic coefficient in all three directions and gravity.

III CFD computations

III.I Lee et al. rotor IGE - CFD Validation

The Lee et al. test case [2] has been computed for two heights above the ground, h/R=1 and h/R=0.5. In both cases, overset grid has been used to model the rotor. No slip and no penetration conditions have been imposed on the ground. Both full rotor domains were computed as unsteady. In both configurations the time step has changed during the simulation, they started with 5deg/timestep for the first two revolutions and then it has been gradually changed to 1deg/time step. The case at h/R=0.5 was computed 4 full rotor revolutions, while the h/R=1 for 6 full rotor revolution, ending the last two with a time step of 0.5 deg/step. CFD analysis of this micro-rotor in OGE has been discussed in [8] comparing with the Ramasamy et al. [7] experimental results. Figure 3 shows the performance validation, in terms of C_T^{IGE}/C_T^{OGE} and C_Q^{IGE}/C_Q^{OGE}. In general, the results show good agreement with the thrust coefficient ratio, showing the expected increase of thrust due to the influence of the ground. In the h/R=0.5 the C_T^{IGE}/C_T^{OGE} is slightly higher with respect to the experiment results and other CFD simulation of the test case performed [30]. The torque coefficient is almost constant with respect to the OGE case, showing C_Q^{IGE}/C_Q^{OGE} near 1. A decrease of the torque coefficient IGE was expected, however a constant torque with an increase of thrust coefficient is an acceptable result for the increased thrust obtained. Outflow profiles have been compared with experimental results using two different scaling. The first was proposed by Lee et al. [2]. They normalized the measured radial velocity with the rotor induced velocity, $v_i = \sqrt{C_T/2}$. On the other hand, it is possible to normalize the radial velocity with v_{max}, the maximum velocity of the outflow, using a jet approach. In Figure 4, the computed time-averaged outflows for h/R=1, at different radial distances, are compared with experiment results. For radial stations closer to the rotor the agreement is better in terms of peak velocity and momentum distribution. However, the agreement worsens at larger radial stations. At r/R=2, the outflow is overestimated from z/R=0.4 to the ground. This can be due to the number of rotor revolutions performed, which may be not enough to have a full settled outflow profile. Using the jet scaling approach, at radial stations closer to rotor, the agreement is better. However, for r/R=2 it is still possible to notice differences in the distribution of the outflow. For the h/R=0.5 the results are shown in figure 5. At radial stations in proximity of the rotor, CFD can predict the outflow with minor differences in the peak value, however at r/R=2 the peak is strongly underestimated, with a different distribution of the momentum along the height above the ground.

IV. Safety Consideration

IV.I Outflows and Forces

Figure 7 shows the obtained outflow, after applying both scaling factors for full-scale aircraft, at two radial stations. Before computing the total force acting on staff personnel, using the PAXman model, some safety considerations can be done. In [31] authors tested the effect of different wind velocities on pedestrians in a wind tunnel. They suggest that under 10 m/s the wind has a very limited effect on people. However at 15 m/s or more, the effect on people may be significant. At such high speed, pedestrians begin to have problems with walking and keeping eyes open. All this can generate risks for non-trained personnel or civilians in proximity to lifting rotors. Results shown in Figure 7 (a) at a radial distance of r/R=1 suggest that the scaled outflow computed in this work may have similar effect to people

in proximity to a lifting rotor, causing some risks. On the other hand, for higher radial distance r/R=2, the outflow velocities drop to safer values. This result may be not accurate, due to the strong underestimation of the peak outflow at this radial station, shown in Figure 5 (c).

Figure 8 shows the PAXman model forces computed for the test cases computed. In general, the forces have their peaks around 1R and 1.5R, after this, they drop quickly and after 2R the forces are almost negligible. In general for all cases, the full area around the rotor can be considered safe in terms of forces acting on ground staff. Comparing different distances above the ground for the same rotor (Figure 8 (a)) it is possible to notice that when the rotor is at h/R=1 it produces higher forces with respect to the h/R=0.5 case. The force distributions over the PAXman height are shown in Figure 9. In Figure 9 (a) the forces are scaled to a light aircraft, while in (b) with a heavy helicopter. Results are in agreement with Figure 8, showing that, at the most of different radial stations, the PAXman forces are stronger when the rotor is at h/R=1 with respect to h/R=0.5.

IV.II Uplift and particles tracking

Figure 10 shows contours of the uplift ratios of the Lee et al. [2] test case, at two different configurations. The rotors were operating at same collective, but at different height above the ground. Contours represent the ratio between the wall friction velocity and the friction threshold. In other worlds, when $u_t/u_t^* > 1$ the particle is uplifted. Results show that the majority of the particles are uplifted in proximity to 1R, however, the uplift halo of h/R=0.5 case is between 1R and 1.5R, while the h/R=0.5 reaches almost 2R. A more detailed analysis shows that when the rotor is closer to the ground, the friction velocity reaches higher values. This is due to the smaller distance between the rotor and the ground, which lead to higher value of induced velocity. Figure 11 shows the particle tracking computed for the Lee et al. test case at h/R=1. Particles with mass were used, and gravity has been taken into account. The flowfield has been scaled as shown previously, with the data of three helicopter weights. Initially, particles are pushed further away from the rotor in all the three cases, however, after 4R it is possible to see the effects of different aircraft. The heaviest helicopter generate an outflow that reingest all the particles uplifted. For the other two cases, some particles have not enough energy to be reingested by the rotor and they reach higher radial distances (more than 10R). Both behaviours can generate risks. When the particles are reingested by the rotor, they can be dangerous for the aircraft and the crew. In this case, the particles generate a cloud around the aircraft, that can lead to a degraded visual environment. Furthermore, particles can be reingested by the helicopter engines or hit the blade damaging it. If the particles are not reingested they are pushed outboard, reaching higher distances. In this case particles, can hit ground personnel or structures. However, in all cases computed in this work, the presence of the particles was reduced beyond 3 rotor diameters.

IV. Conclusions and Future Work

The CFD performance comparisons with the Lee et al. experimental results [2] are in broad agreement for rotor loads and outflow, however,there are some differences in the prediction of the torque coefficient and radial velocity at radial stations further away from the rotor. These differences can be important when results are used to evaluate forces and particle paths for safety. Using the proposed scaling methods, the outflow produced by the two rotors have been analysed. Comparing the radial velocity with the results in [31], the outflow produced by the rotors may to cause risk to people in proximity to the rotor. Using the PAXman model, it is possible to compute the forces on ground personnel. In terms of computed forces, the nearby area of the rotor is safe for the majority of the cases considered. There are, however, differences in terms of accepted thresholds. In [31], authors defined thresholds for civilian pedestrians. On the other hand, the PAXman model was developed for military personnel, and includes considerations on weight, size, age, health, protective clothing and tasks. This allows trained personnel to suffer less at strong outflow velocities. In general, forces and outflow velocities drop to safe values after 2R, and it is possible consider that 3 rotor diameters, as used for wake encounters [10] [9], is a suitable safe distance for outflow and forces on personnel. On the other hand, the presence of particle in the flowfield cannot be excluded beyond the 3 rotor diameters distance. Particles can reach high radial distances from the rotor, causing damage to ground personnel and structures, furthermore reingested particles can generate DVE conditions like brownout, which is a severe source of risk for the crew and the aircraft.

Acknowledgments

This project has received funding from the European Union's H2020 research and innovation programme under the Marie Sktodowska-Curie grant agreement No 721920

Bibliography

[1] Silva, M., and Riser, R., "CH-47D tandem rotor outwash survey," *AHS 67th Annual Forum,Virginia Beach, Virginia, USA,*, 2011, p. 221.

[2] Lee, T. E., Leishman, J. G., and Ramasamy, M., "Fluid dynamics of interacting blade tip vortices with a ground plane," *Journal of the American Helicopter Society*, Vol. 55, No. 2, 2010, pp. 22005–22005.

[3] Milluzzo III, J. I., and Leishman, J. G., "Vortical sheet behavior in the wake of a rotor in ground effect," *AIAA Journal*, Vol. 55, No. 1, 2016, p. 24.

[4] Glauert, M., "The wall jet," *Journal of Fluid Mechanics*, Vol. 1, No. 6, 1956, pp. 625–643.

[5] Preston, J. R., Troutman, S., Keen, E., Silva, M., Whitman, N., Calvert, M., Cardamone, M., Moulton, M., and Ferguson, S. W., "Rotorwash Operational Footprint Modeling," Tech. rep., Missile Research Development and Engineering Center Redstone Arsenal AL Missile Guidance directorate, 2014.

[6] Taskgroup, R., "Rotary-wing brownout mitigation: technologies and training," *Tech. Rep. RTO-TR-HFM-162, NATO Sci. Technol. Org.*, 2010.

[7] Ramasamy, M., Johnson, B., and Leishman, J. G., "Understanding the Aerodynamic Efficiency of a Hovering Micro-Rotor," *Journal of the American Helicopter Society*, Vol. 53, No. 4, 2008, pp. 412–428.

[8] Rovere, F., Barakos, G., and Steijl, R., "CFD validation of a micro-rotor in grond effect," *45th European Rotorcraft Forum, Warsaw*, CFAS, 2019.

[9] Jimenez-Garcia, A., Barakos, G., Treve, V., Rooseleer, F., Cappellazzo, V., and Graham, R., "Helicopter Wake Encounters in the Context of RECAT-EU," *43th European Rotorcraft Forum, Milan*, CFAS, 2017.

[10] CAA, "CAP 490: Manual of Air Traffic Services Part 1," 2015.

[11] Steijl, R., Barakos, G., and Badcock, K., "A framework for CFD analysis of helicopter rotors in hover and forward flight," *International journal for numerical methods in fluids*, Vol. 51, No. 8, 2006, pp. 819–847.

[12] Lawson, S., Woodgate, M., Steijl, R., and Barakos, G., "High performance computing for challenging problems in computational fluid dynamics," *Progress in Aerospace Sciences*, Vol. 52, 2012, pp. 19–29.

[13] Osher, S., and Chakravarthy, S., "Upwind schemes and boundary conditions with applications to Euler equations in general geometries," *Journal of Computational Physics*, Vol. 50, No. 3, 1983, pp. 447–481.

[14] Roe, P. L., "Approximate Riemann solvers, parameter vectors, and difference schemes," *Journal of computational physics*, Vol. 43, No. 2, 1981, pp. 357–372.

[15] Van Leer, B., "Towards the ultimate conservative difference scheme. V. A second-order sequel to Godunov's method," *Journal of computational Physics*, Vol. 32, No. 1, 1979, pp. 101–136.

[16] Van Albada, G., Van Leer, B., and Roberts, W., "A comparative study of computational methods in cosmic gas dynamics," *Upwind and High-Resolution Schemes*, Springer, 1997, pp. 95–103.

[17] Jarkowski, M., Woodgate, M., Barakos, G., and Rokicki, J., "Towards consistent hybrid overset mesh methods for rotorcraft CFD," *International Journal for Numerical Methods in Fluids*, Vol. 74, No. 8, 2014, pp. 543–576.

[18] Steijl, R., and Barakos, G., "Sliding mesh algorithm for CFD analysis of helicopter rotor–fuselage aerodynamics," *International journal for numerical methods in fluids*, Vol. 58, No. 5, 2008, pp. 527–549.

[19] Menter, F. R., "Two-equation eddy-viscosity turbulence models for engineering applications," *AIAA journal*, Vol. 32, No. 8, 1994, pp. 1598–1605.

[20] Bagnold, R., "The physics of blown sand and desert dunes. London: Methuen." 1941.

[21] Greeley, R., and Iversen, J. D., *Wind as a geological process: on Earth, Mars, Venus and Titan*, Vol. 4, CUP Archive, 1987.

[22] Shao, Y., and Lu, H., "A simple expression for wind erosion threshold friction velocity," *Journal of Geophysical Research: Atmospheres*, Vol. 105, No. D17, 2000, pp. 22437–22443.

[23] Shao, Y., and Li, A., "Numerical Modelling of Saltation in the Atmospheric Surface Layer," *Boundary-Layer Meteorology*, Vol. 91, No. 2, 1999, pp. 199–225.

[24] Tanner, P. E., "Photogrammetric characterization of a brownout cloud," *67th Annual Forum of the American Helicopter Society, Virginia Beach, VA*, 2011.

[25] Syal, M., Govindarajan, B., and Leishman, J., "Mesoscale sediment tracking methodology to analyze brownout cloud developments," *66th Annual Forum of the American Helicopter Society, Phoenix, AZ*, 2010, pp. 11–13.

[26] Alfred, J., Celi, R., and Leishman, J. G., "Flight Path Optimization for Brownout Mitigation Using a High-Fidelity Simulation Model," *Journal of the American Helicopter Society*, Vol. 62, No. 3, 2017, pp. 1–15.

[27] Wachspress, D., Whitehouse, G., Keller, J., Yu, K., Gilmore, P., Dorsett, M., and McClure, K., "A high fidelity brownout model for real-time flight simulations and trainers," 2009, pp. 278–301.

[28] Phillips, C., Kim, H. W., and Brown, R. E., "The flow physics of helicopter brownout," *66th American Helicopter Society Forum: Rising to New Heights in Vertical Lift Technology*, 2010.

[29] Ghosh, S., Lohry, M. W., and Rajagopalan, R. G., "Rotor configurational effect on rotorcraft brownout," *28th AIAA Applied Aerodynamics Conference*, 2010, p. 4238.

[30] Kalra, T. S., Lakshminarayan, V. K., and Baeder, J. D., "Cfd validation of micro hovering rotor in ground effect," *American Helicopter Society 66th Annual Forum Proceedings, Phoenix, Arizona USA*, Citeseer, 2010.

[31] Murakami, S., and Deguchi, K., "New criteria for wind effects on pedestrians," *Journal of Wind Engineering and Industrial Aerodynamics*, Vol. 7, No. 3, 1981, pp. 289–309.

[32] "Vertipedia," `https://vertipedia.vtol.org/`, Accessed: 23-09-2019.

a0	4.30939e-01
a1	-4.63972e-02
a2	-1.39649e-01
a3	1.37545e-01
a4	-2.48764e-02
a5	-5.49253e-04
a6	2.21653e-04
a7	-4.18444e-05
a8	1.45194e-05
a9	-7.80009e-08
a10	-1.89822e-07

Table 1 Polynomial coefficients used for the curve in Figure 1**.**

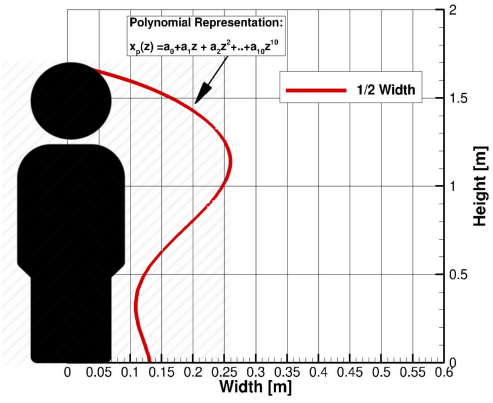

Fig. 1 PAXman model [5]**.**

Category	MTOW (kg)	R (m)	V_{tip} (m/s)	C_T
Light	3000	5.5	220	0.009
Medium	5400	7	220	0.0116
Heavy	11000	8.1	220	0.0176

Table 2 Helicopters technical data [32]**.**

$\rho_p(kg/m^3)$	$d_p\ (\mu m)$	C_D	B
1400	2.5	1.048	0.0023

Table 3 Properties of particles used in this work for particle tracking.

$\rho_p(kg/m^3)$	$d_p\ (\mu m)$	$u_t^*(m/s)$
2160	25	0.35

Table 4 Properties of particles used in this work for the uplift model.

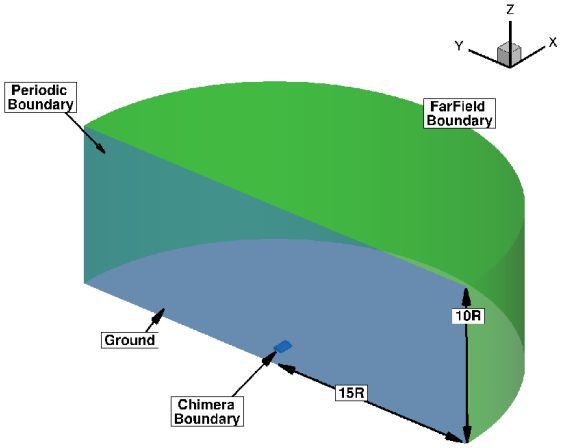

Fig. 2 CFD domains for the Lee et al. [2].

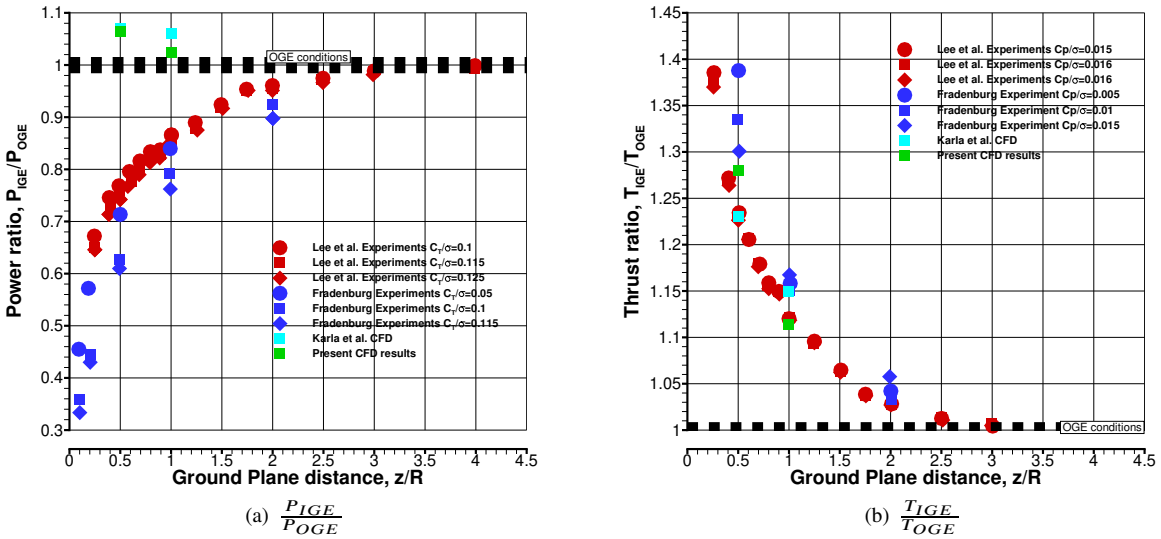

(a) $\frac{P_{IGE}}{P_{OGE}}$ (b) $\frac{T_{IGE}}{T_{OGE}}$

Fig. 3 Power and trust ratios for the Lee et al. rotor [2] [30].

Mesh	1	2	3	4	5	6
Grid Type	Chimera	Chimera	Chimera	Chimera	Chimera	Chimera
Component	Blade	Background	Hub	Composite	Background	Composite
Collective angle (deg)	12			12		
N blades	2			2		
Mesh components				1+2+3		1+3+4
Scaling factor	c	c	c	c	c	c
Number of Points (Million)	19 M	19.9 M	0.4 M	39.3 M	19.9 M	39.3 M
Distance from the ground						
Blade plane		0.5R		0.5	1R	1R
Top of domain		10R		10R	10R	10R
Side of domain		15R		15R	15R	15R

Table 5 CFD grids for the Lee et al. [2] rotor.

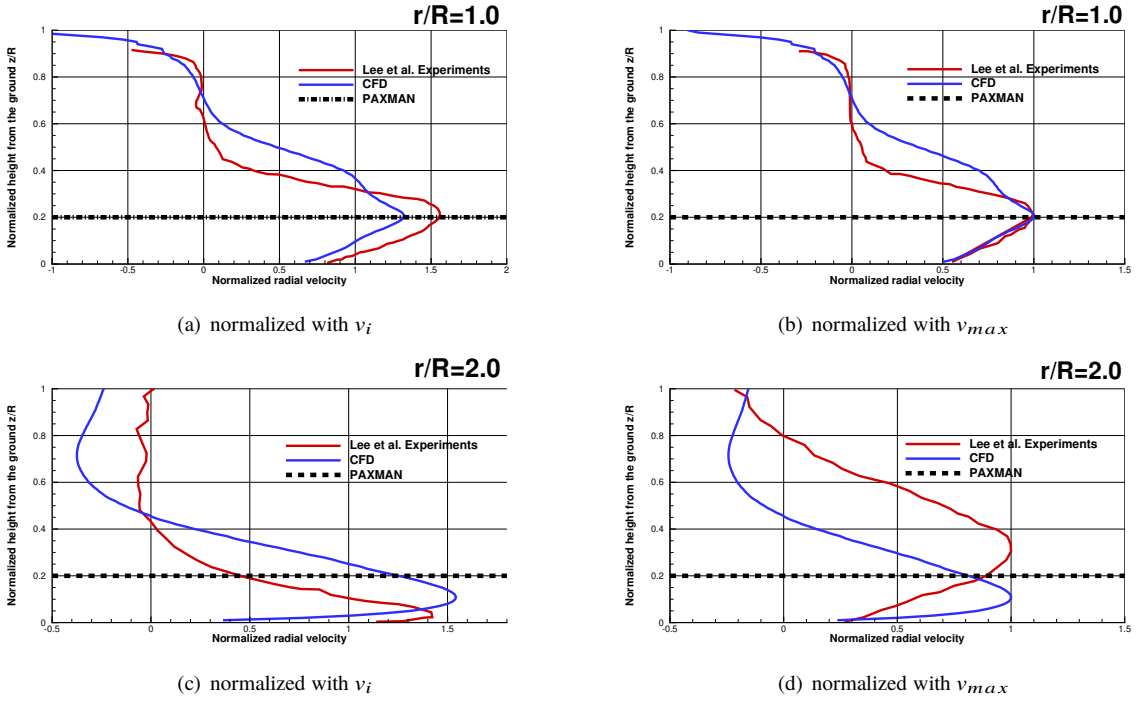

(a) normalized with v_i

(b) normalized with v_{max}

(c) normalized with v_i

(d) normalized with v_{max}

Fig. 4 Outwash at h/R=1, normalized with v_i (left) and v_{max} (right). The Lee et al. rotor [2] was operating at $Re_{tip} = 35000$, $M_{tip} = 0.08$, $\theta_{75} = 12deg$ and $C_T = 0.03$.

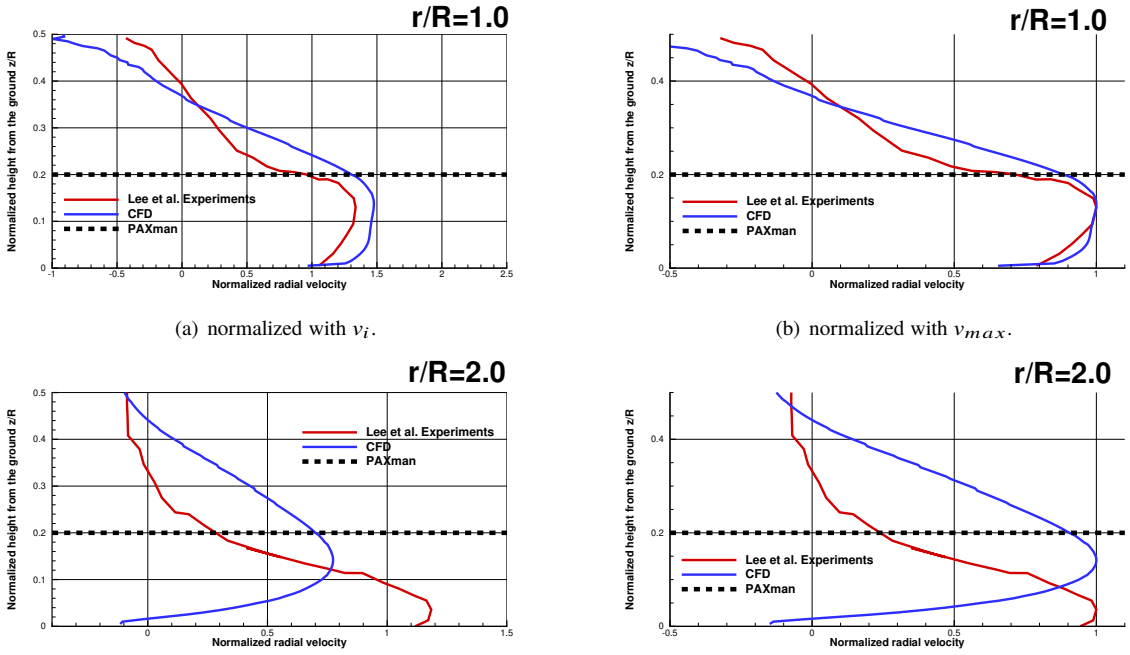

(a) normalized with v_i.

(b) normalized with v_{max}.

(c) normalized with v_i.

(d) normalized with v_{max}.

Fig. 5 Outwash at h/R=0.5, normalized with v_i (left) and v_{max} (right). The Lee et al. rotor [2] was operating at $Re_{tip} = 35000$, $M_{tip} = 0.08$, $\theta_{75} = 12deg$ and $C_T = 0.035$.

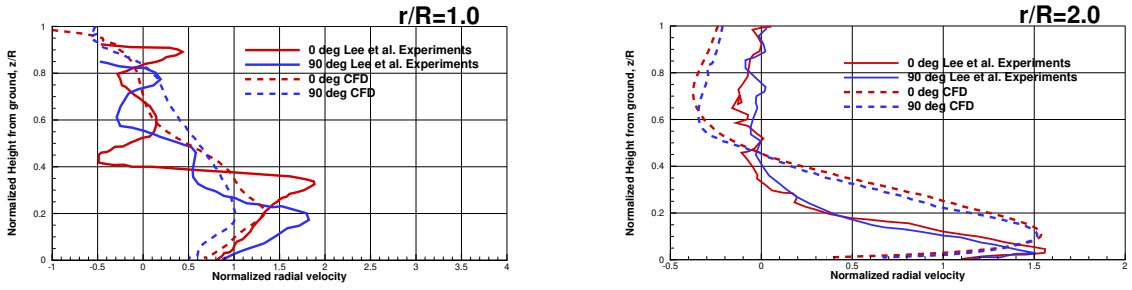

(a) r/R=1.0

(b) r/R=2.0

Fig. 6 Velocity profiles normalized with v_i at two different azimuth angles: 0 and 90 deg. The Lee et al. rotor [2] was operating at h/R=1, $Re_{tip} = 35000$, $M_{tip} = 0.08$, $\theta_{75} = 12deg$ and $C_T = 0.03$.

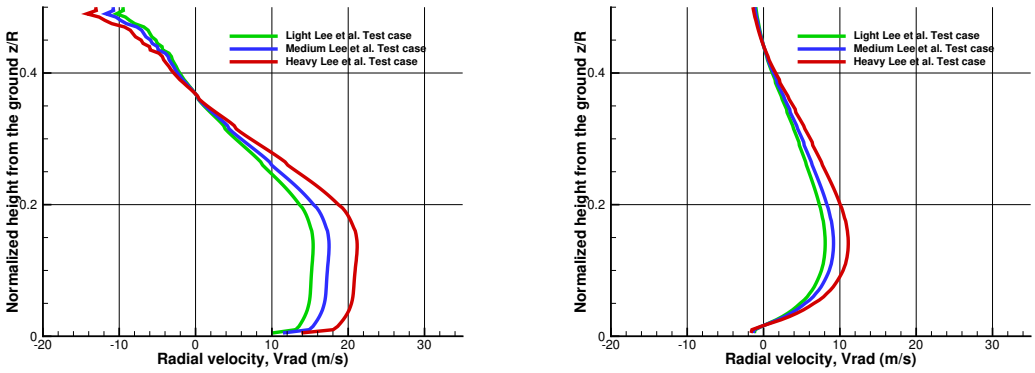

(a) r/R=1 (b) r/R=2

Fig. 7 Outflows after appling the scaling factors. Lee et al. rotor [2] was operating at h/R=0.5, Re_{tip}=32000, $Re_{tip} = 0.08$, $\theta_{75} = 12deg$ and $C_T = 0.035$. A scaling of $V_{tip} = 220m/s$ was used for all weight categories, C_T values for full scale given in Table 2.

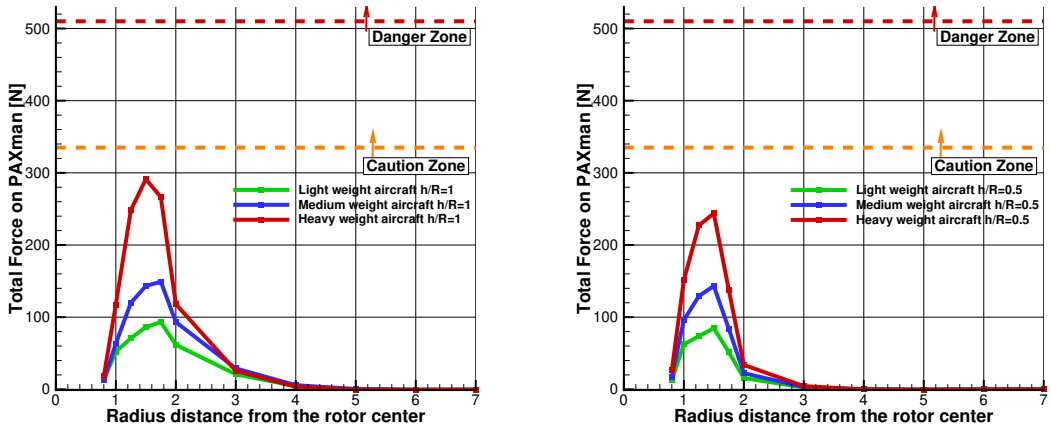

(a) Total radial forces, Lee et al. test case, h/R=1 and $C_T = 0.03$ (b) Total radial forces, Lee et al. test case, h/R=0.5 and $C_T = 0.035$

Fig. 8 Paxman model total forces. Lee et al. rotor [2] was operating at $Re_{tip} = 35000$, $M_{tip} = 0.08$ and $\theta_{75} = 12deg$. A scaling of $V_{tip} = 220m/s$ was used for all weight categories, and the C_T values for full scale are given in Table 2.

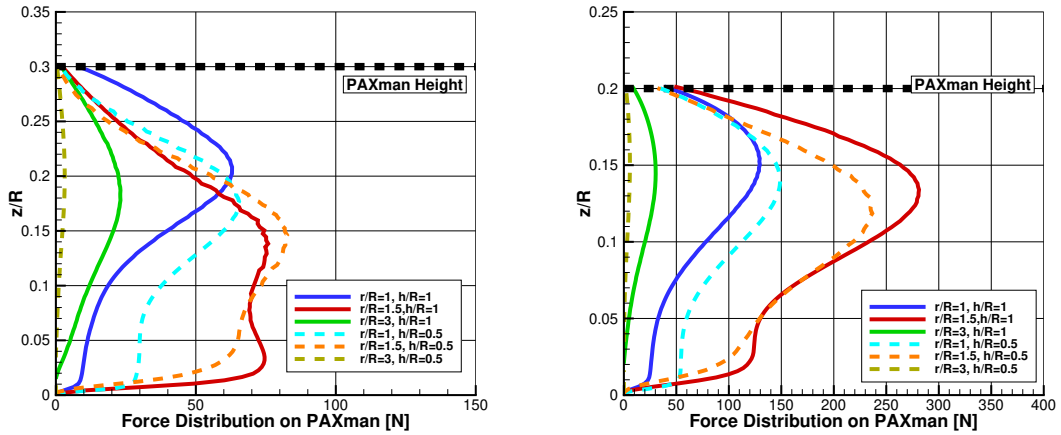

(a) Paxman force distribution scaled for light weight aircraft (b) Paxman force distribution scaled for heavy weight aircraft

Fig. 9 Comparison of PAXman model forces distribution. Lee et al. rotor [2] was operating at h/R=0.5, $Re_{tip} = 35000$, $M_{tip} = 0.08$ and $\theta_{75} = 12deg$. A scaling of $V_{tip} = 220m/s$ was used for all weight categories, and the C_T values for full scale are given in Table 2.

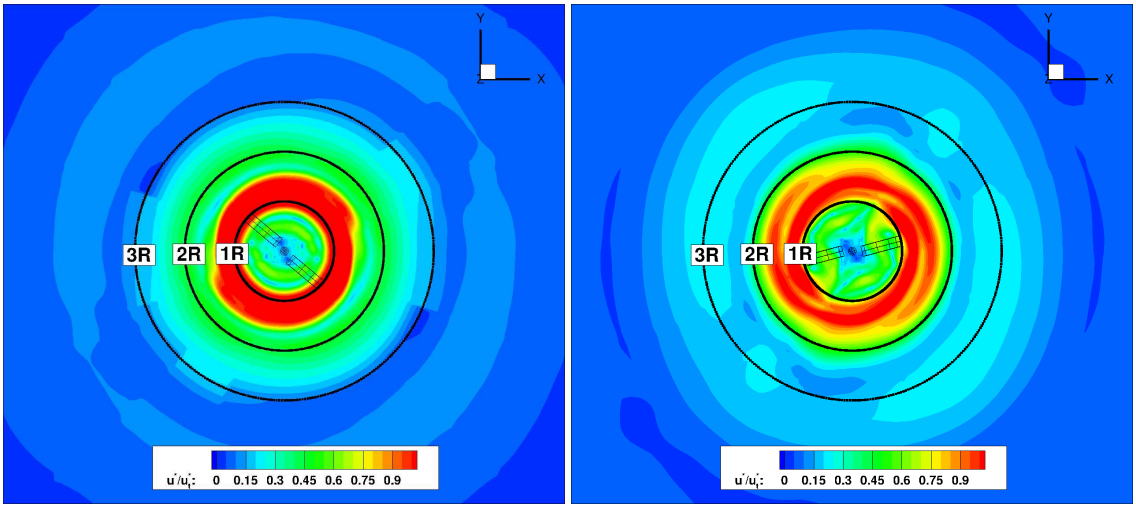

(a) Lee et al. test case, h/R=0.5 and $C_T = 0.035$ (b) Lee et al. test case, h/R=1 and $C_T = 0.03$

Fig. 10 Uplift ratio, u_t^*/u_t for particles with $u_t = 0.35$ m/s. Lee et al. rotor [2] was operating at h/R=0.5, $Re_{tip} = 35000$, $M_{tip} = 0.08$ and $\theta_{75} = 12deg$.

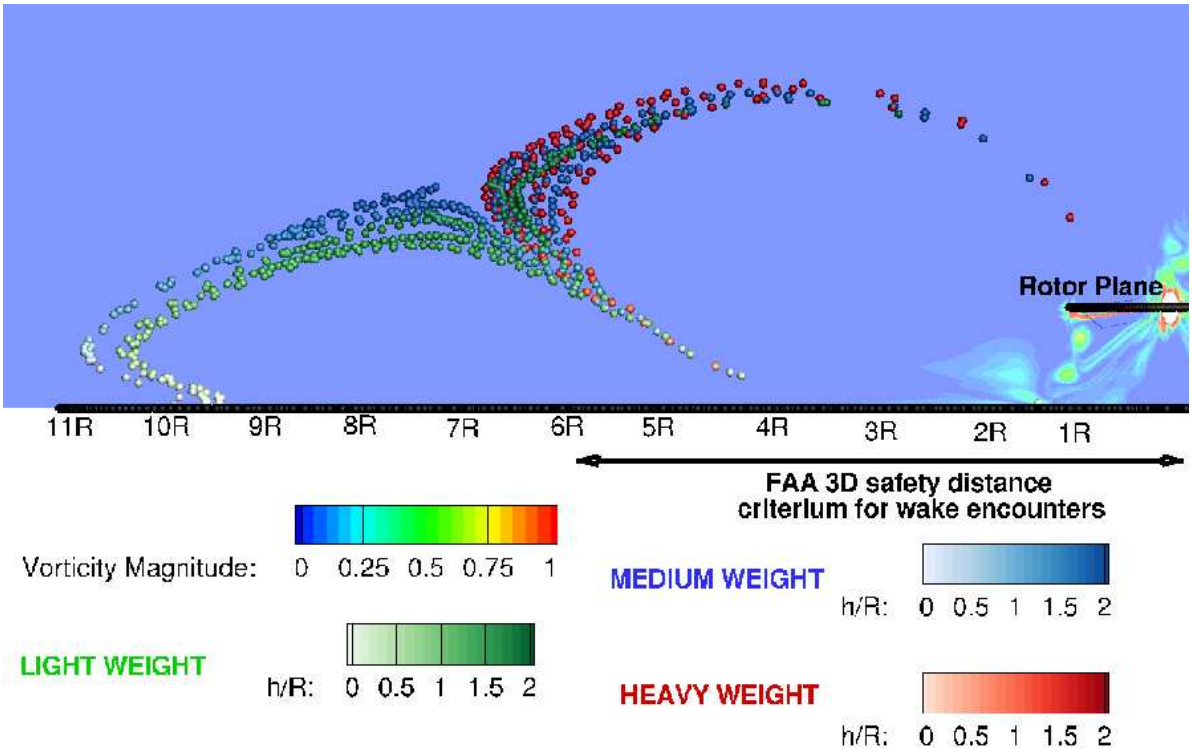

Fig. 11 Particle tracking, using velocities scaled with three weight categories of aircraft: light (green), medium (blue) and heavy (red). A tip velocity V_{tip} = 220 m/s and MTOW were used. Particles has B=0.0023 and gravity. The rotor was operating at $\theta_{75} = 12deg$, $Re_{tip} = 35000$, $M_{tip} = 0.08$, $h/R = 1$ and $C_T = 0.03$. Contours correspond to the vorticity magnitude and the FAA wake separation distance is shown for comparison [10].